

Quantum impurities and angular momentum in a many-body system: analytical and numerical approaches

Giacomo Bighin

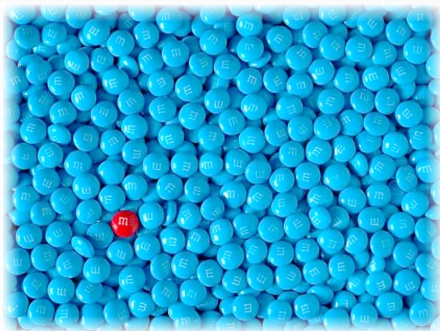
March 6th, 2025

Quantum impurities

One particle (or a few particles)
interacting with a many-body
environment.

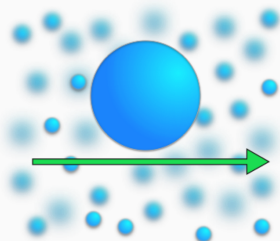
- Condensed matter
- Chemistry
- Ultracold atoms: tunable interaction
with either bosons or fermions.

A prototype of a many-body system.
How are the properties of the particle
modified by the interaction?



Quantum impurities

Structureless impurity: translational degrees of freedom/linear momentum exchange with the bath. Most common cases: electron in a solid, atomic impurities in a BEC.



Quantum impurities

Structureless impurity: translational degrees of freedom/linear momentum exchange with the bath. Most common cases: **electron in a solid**, atomic impurities in a BEC.

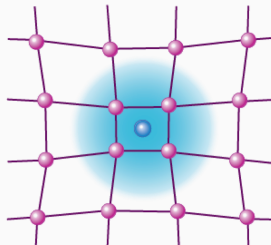


Image from: F. Chevy, Physics 9, 86.

Quantum impurities

Structureless impurity: translational degrees of freedom/linear momentum exchange with the bath. Most common cases: electron in a solid, **atomic impurities in a BEC.**

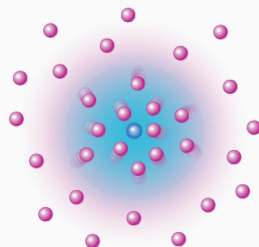


Image from: F. Chevy, Physics 9, 86.

Quantum impurities

Structureless impurity: translational

degrees of freedom
exchange with
cases: electron
impurities in a

Both these scenarios can be formalized in terms
of **quasiparticles** using the **polaron** and the Fröh-
lich Hamiltonian.

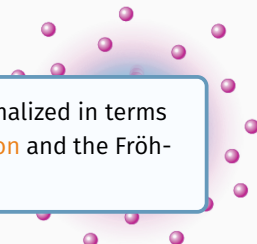


Image from: F. Chevy, Physics 9, 86.

Quantum impurities

Structureless impurity: translational degrees of freedom/linear momentum exchange with the bath. Most common cases: electron in a solid, atomic impurities in a BEC.

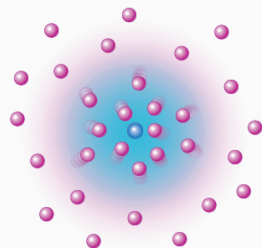
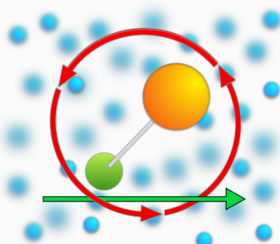


Image from: F. Chevy, Physics 9, 86.



Composite impurity, e.g. a diatomic molecule: translational and rotational degrees of freedom/linear and angular momentum exchange.

Quantum impurities

Structureless impurity: translational degrees of freedom/linear momentum exchange with the bath. Most common cases: electron in a solid, atomic impurities in a BEC.

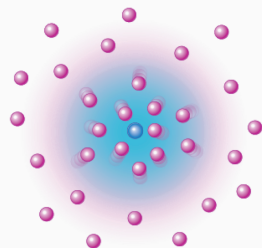
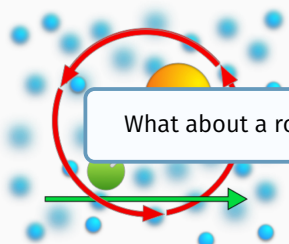


Image from: F. Chevy, Physics 9, 86.



What about a rotating particle?

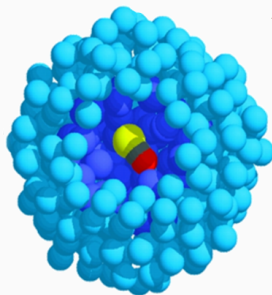
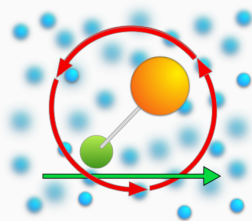
Composite impurity, e.g. a diatomic molecule. It can have both rotational and angular momentum exchange.

In this talk

Rotating quantum impurities as quasiparticles, and diagrammatics

Molecules in ^4He nanodroplets

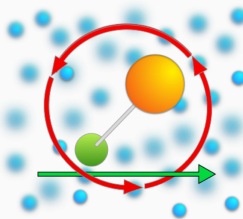
Ultra-cold atoms: an impurity in a Bose-Bose mixture



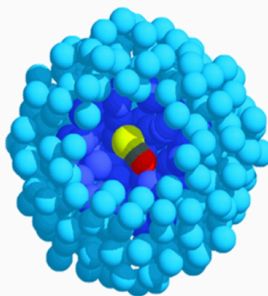
Images from S. Grebenev *et al.*, Science **279**, 2083 (1998) and from C.R. Cabrera's Ph.D. thesis.

In this talk

Rotating quantum impurities as quasiparticles, and diagrammatics



Molecules in ^4He nanodroplets



Ultra-cold atoms: an impurity in a Bose-Bose mixture



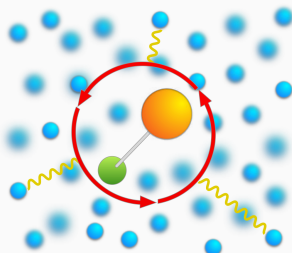
Images from S. Grebenev et al., Science 279, 2083 (1998) and from C.R. Cabrera's Ph.D. thesis.

The angulon Hamiltonian

A composite impurity in a bosonic environment can be described by the **angulon Hamiltonian**¹²³⁴ (angular momentum basis: $\mathbf{k} \rightarrow \{k, \lambda, \mu\}$):

$$\hat{H} = \underbrace{B\hat{\mathbf{J}}^2}_{\text{molecule}} + \underbrace{\sum_{k\lambda\mu} \omega_k \hat{b}_{k\lambda\mu}^\dagger \hat{b}_{k\lambda\mu}}_{\text{phonons}} + \underbrace{\sum_{k\lambda\mu} U_\lambda(k) \left[Y_{\lambda\mu}^*(\hat{\theta}, \hat{\phi}) \hat{b}_{k\lambda\mu}^\dagger + Y_{\lambda\mu}(\hat{\theta}, \hat{\phi}) \hat{b}_{k\lambda\mu} \right]}_{\text{molecule-phonon interaction}}$$

- Linear molecule
- Derived rigorously for a molecule in a weakly-interacting BEC¹
- Phenomenological model for a molecule in any kind of bosonic bath³



¹R. Schmidt and M. Lemeshko, Phys. Rev. Lett. **114**, 203001 (2015).

²R. Schmidt and M. Lemeshko, Phys. Rev. X **6**, 011012 (2016).

³M. Lemeshko, Phys. Rev. Lett. **118**, 095301 (2017).

⁴Yu. Shchadilova, "Viewpoint: A New Angle on Quantum Impurities", Physics **10**, 20 (2017).

How to tackle the Hamiltonian

Variational Ansatz

Expansion in bath excitations (cfr. Chevy Ansatz for polarons):

$$|\Psi\rangle \approx |\bullet\circlearrowleft\rangle_{\text{imp}} \otimes |0\rangle_{\text{bos}} + |\bullet\circlearrowleft\rangle_{\text{imp}} \otimes |1\rangle_{\text{bos}} + \dots$$

plus some variational coefficients, to optimize by minimizing energy.

See for instance: R. Schmidt and M. Lemeshko, Phys. Rev. Lett. **114**, 203001 (2015).

How to tackle the Hamiltonian

Feynman diagrams

Here I will show how the problem can be described in terms of Feynman diagrams, and how Feynman diagrams can be systematically summed to arbitrarily high order with diagrammatic Monte Carlo.

Diagrammatics for molecular rotations

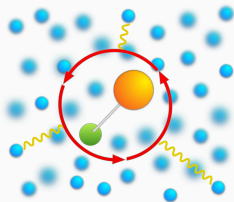
$$\begin{aligned} \text{---} &= \text{---} + \text{---} + \\ &+ \text{---} + \dots \end{aligned}$$

The diagram illustrates the decomposition of a total molecular rotation into its components. A thick black horizontal line on the left is equated to a sum of simpler diagrams. The first term is a thin grey horizontal line. The second term is a thin grey horizontal line with a dashed blue semicircle arc above it, starting and ending at red dots on the line. The third term is a thin grey horizontal line with a dashed blue quarter-circle arc above it, also starting and ending at red dots. This pattern continues with additional terms, each consisting of a thin grey horizontal line with a dashed blue arc above it, starting and ending at red dots.

Diagrammatics for molecular rotations

$$\begin{array}{c} \text{---} = \text{---} + \text{---} \\ \text{---} + \text{---} + \dots \end{array}$$

How do we describe **molecular rotations** with Feynman diagrams? How does angular momentum enter this picture?

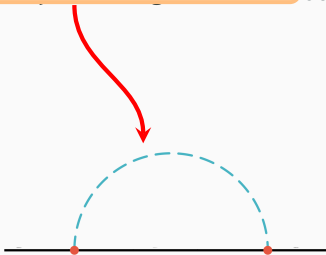
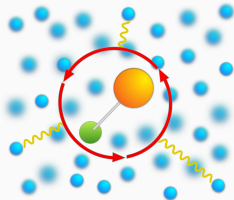


Diagrammatics for molecular rotations

$$\text{---} = \text{---} + \text{---} + \\ + \text{---} + \dots$$

How does **angular momentum** enter here?

How do we describe **molecular** rotation? Does angular momentum enter this picture?

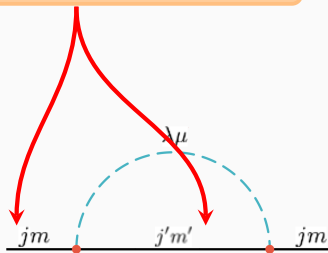
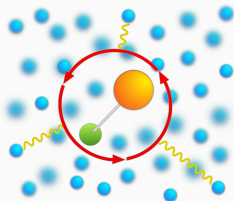


Diagrammatics for molecular rotations

$$\text{---} = \text{---} + \text{---} + \dots$$
$$+ \text{---} + \dots$$

Write on each line j, m , that is angular momentum and projection along z axis.

How do we describe **molecular** rotation? Does angular momentum enter this picture?

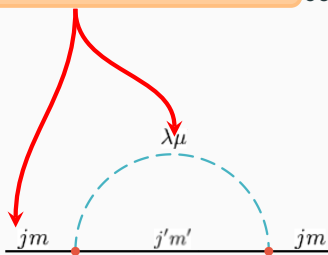
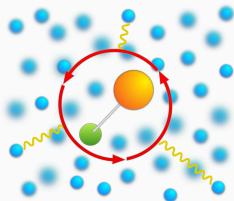


Diagrammatics for molecular rotations

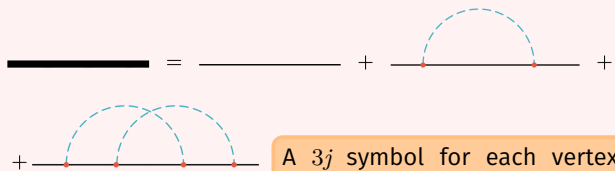
$$\text{---} = \text{---} + \text{---} + \dots$$
$$+ \text{---} + \dots$$

Angular momentum dependent propagators: $G_{0,j}$ and D_j

How do we describe molecular rotation? Does angular momentum enter this picture?



Diagrammatics for molecular rotations

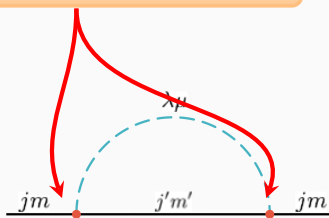
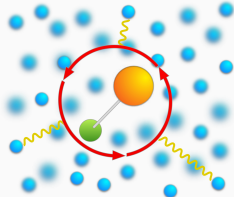


A $3j$ symbol for each vertex, enforcing angular momentum conservation.

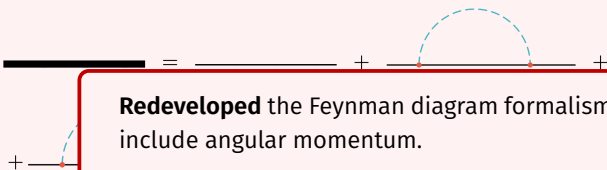
$$\left(\begin{array}{ccc} j_1 & j_2 & j_3 \\ m_1 & m_2 & m_3 \end{array} \right)$$

oes

How do we describe **molecular** angular momentum enter this



Diagrammatics for molecular rotations

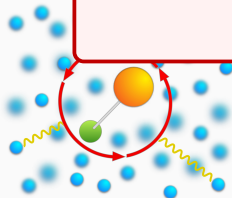


Redeveloped the Feynman diagram formalism to include angular momentum.

Opens up the possibility of using several tools from many-body theory.

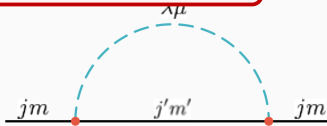
For instance: Dyson equation

$$G = \frac{1}{G_0^{-1} - \Sigma}$$



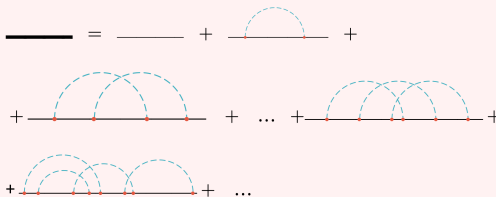
w does

How do we d
angular mom



Diagrammatic Monte Carlo

Numerical technique for sampling over all Feynman diagrams¹.



- **DiagMC idea:** set up a stochastic process sampling among all diagrams¹
- **Configuration space:** diagram topology, phonons internal variables, times, etc... Number of variables varies with the topology!
- **How:** ergodicity, detailed balance $w_1 p(1 \rightarrow 2) = w_2 p(2 \rightarrow 1)$
- **Result:** each configuration is visited with probability \propto its weight.

Up to now: **structureless** particles (Fröhlich polaron, Holstein polaron), or particles with a very **simple internal structure** (e.g. spin $1/2$). Now: **molecules**.

¹N. V. Prokof'ev and B. V. Svistunov, Phys. Rev. Lett. **81**, 2514 (1998).

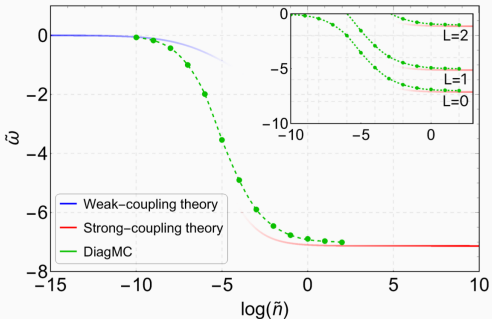
²GB, T.V. Tscherbul, M. Lemeshko, Phys. Rev. Lett. **121**, 165301 (2018).

Diagrammatic Monte Carlo: results

The ground-state energy of the angulon Hamiltonian obtained using DiagMC¹ as a function of the dimensionless bath density, \tilde{n} , compared with the weak-coupling theory² and the strong-coupling theory³.

The energy and quasiparticle weight are obtained by fitting the long-imaginary-time behaviour of G_j as $G_j(\tau) = Z_j \exp(E_j \tau)$.

Inset: energy of the $L = 0, 1, 2$ states.



A numerically exact technique for studying molecules. Bridging different communities (solid state, chemistry) with far reaching consequences⁴.

¹GB, T.V. Tscherbul, M. Lemeshko, Phys. Rev. Lett. 121, 165301 (2018).

²R. Schmidt and M. Lemeshko, Phys. Rev. Lett. **114**, 203001 (2015).

³R. Schmidt and M. Lemeshko, Phys. Rev. X **6**, 011012 (2016).

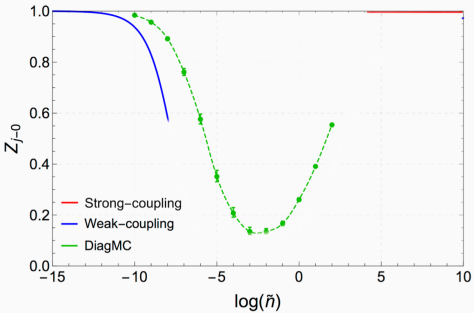
⁴GB, Q.P. Ho, T.V. Tscherbul, M. Lemeshko, Phys. Rev. B **108**, 045115 (2023).

Diagrammatic Monte Carlo: results

The ground-state energy of the angulon Hamiltonian obtained using DiagMC¹ as a function of the dimensionless bath density, \tilde{n} , compared with the weak-coupling theory² and the strong-coupling theory³.

The energy and quasiparticle weight are obtained by fitting the long-imaginary-time behaviour of G_j as $G_j(\tau) = Z_j \exp(E_j \tau)$.

Inset: energy of the $L = 0, 1, 2$ states.



A numerically exact technique for studying molecules. Bridging different communities (solid state, chemistry) with far reaching consequences⁴.

¹GB, T.V. Tscherbul, M. Lemeshko, Phys. Rev. Lett. **121**, 165301 (2018).

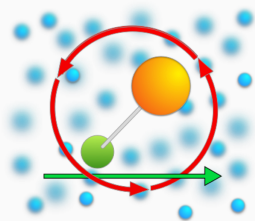
²R. Schmidt and M. Lemeshko, Phys. Rev. Lett. **114**, 203001 (2015).

³R. Schmidt and M. Lemeshko, Phys. Rev. X **6**, 011012 (2016).

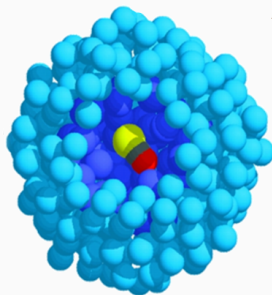
⁴GB, Q.P. Ho, T.V. Tscherbul, M. Lemeshko, Phys. Rev. B **108**, 045115 (2023).

In this talk...

Rotating quantum impurities as quasiparticles, and diagrammatics



Molecules in ^4He nanodroplets



Ultra-cold atoms: an impurity in a Bose-Bose mixture



Images from S. Grebenev et al., Science 279, 2083 (1998) and from C.R. Cabrera's Ph.D. thesis.

Molecules in helium nanodroplets

A molecular impurity embedded into a helium nanodroplet: a controllable system to explore angular momentum redistribution in a many-body environment.

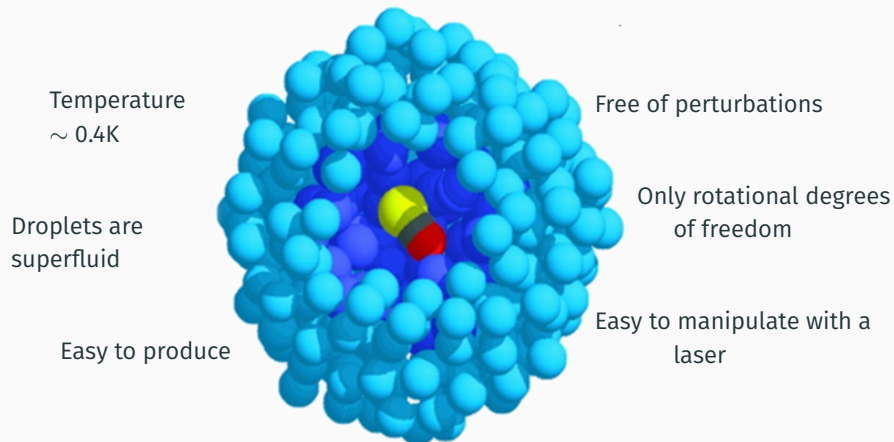
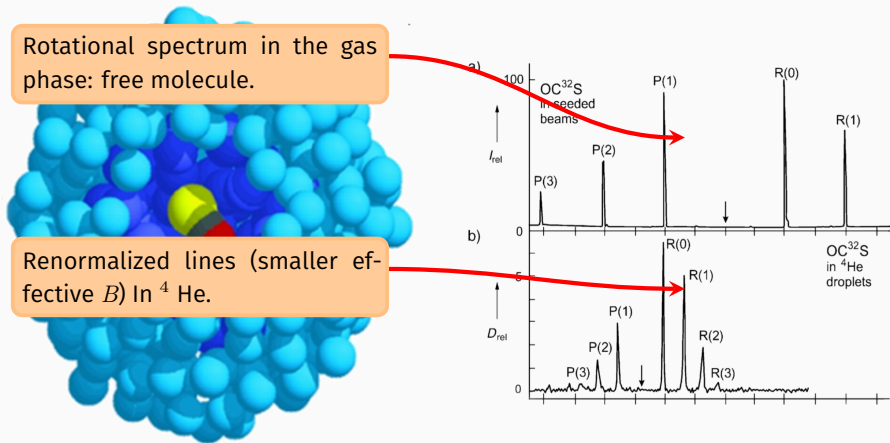


Image from: S. Grebenev *et al.*, Science **279**, 2083 (1998).

Rotational spectrum of molecules in He nanodroplets

Molecules embedded into helium **nanodroplets**: rotational spectrum



Images from: S. Grebenev *et al.*, Science **279**, 2083 (1998). and J.P. Toennies and A.F. Vilesov, Angew. Chem. Int. Ed. **43**, 2622 (2004).

Dynamical alignment of molecules in helium nanodroplets

Dynamical alignment experiments (Stapelfeldt group, Aarhus University):

- **Kick** pulse, aligning the molecule.
- **Probe** pulse, destroying the molecule.
- Fragments are imaged, reconstructing alignment as a function of time.
- Averaging over multiple realizations, and varying the time between the two pulses, one gets

$$\langle \cos^2 \hat{\theta}_{2D} \rangle(t)$$

with

$$\cos^2 \hat{\theta}_{2D} \equiv \frac{\cos^2 \hat{\theta}}{\cos^2 \hat{\theta} + \sin^2 \hat{\theta} \sin^2 \hat{\phi}}$$

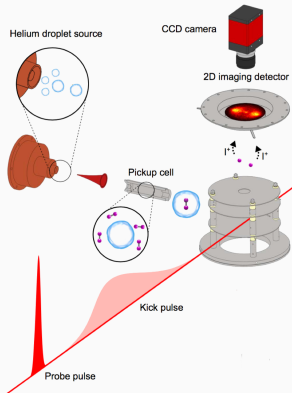
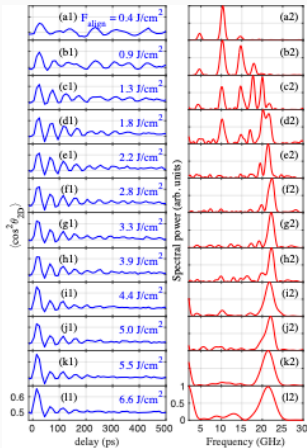


Image from: B. Shepperson et al.,
Phys. Rev. Lett. **118**, 203203 (2017).

Rotational coherence spectroscopy of molecules in helium nanodroplets

Let's look at the alignment traces for CS_2 for different value of the fluence, as well as their Fourier transform.



- The Fourier transform $\langle \cos^2 \hat{\theta}_{2D} \rangle(t)$ is dominated $E_L - E_{L-2}$ for all L 's.
- A new kind of “rotational spectroscopy”. Investigating higher states than conventional IR spectroscopy.
- Unknown oscillation period of $\sim 50\text{ps}$, corresponding to a peak at around 20 GHz in the power spectrum.
- The “renormalized rotational constant” picture here is not enough! Note that

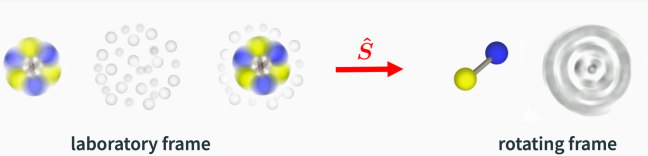
$$E_L = B^* L(L+1) \implies E_L - E_{L-2} \propto BL$$

and this does not explain the 20 GHz peak.

¹A.S. Chatterley, ..., GB, et al., Phys. Rev. Lett. **125**, 013001 (2020).

Canonical transformation

A canonical transformation brings us to a frame of reference co-moving with the molecule (cfr. the Lee-Low-Pines transformation for the polaron).



$$\hat{H} = B(\hat{\mathbf{L}} - \hat{\Lambda})^2 + \sum_{k\lambda\mu} \omega_k \hat{b}_{k\lambda\mu}^\dagger \hat{b}_{k\lambda\mu} + \sum_{k\lambda} V_\lambda(k) [\hat{b}_{k\lambda 0}^\dagger + \hat{b}_{k\lambda 0}]$$

To further simplify the problem we consider a single mode carrying energy ω , fixed at the roton energy, and carrying angular momentum λ . The molecule-solvent interaction strength u is kept as a phenomenological parameter to be adjusted.

$$\hat{H} = B(\hat{\mathbf{L}} - \hat{\Lambda})^2 + \omega \sum_{\lambda\mu} \hat{b}_{\lambda\mu}^\dagger \hat{b}_{\lambda\mu} + u(\hat{b}_{\lambda 0}^\dagger + \hat{b}_{\lambda 0})$$

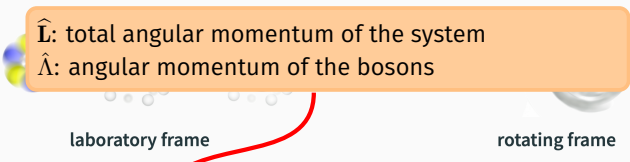
¹I.N. Cherepanov, GB, et al., Phys. Rev. A **104**, L061303 (2021).⁴

²I.N. Cherepanov, GB, et al., New J. Phys. **24**, 075004 (2022).

³R. Schmidt and M. Lemeshko, Phys. Rev. X **6**, 011012 (2016).

Canonical transformation

A canonical transformation brings us to a frame of reference co-moving with the molecule (cfr. the Lee-Low-Pines transformation for the polaron).



$$\hat{H} = B(\hat{\mathbf{L}} - \hat{\Lambda})^2 + \sum_{k\lambda\mu} \omega_k \hat{b}_{k\lambda\mu}^\dagger \hat{b}_{k\lambda\mu} + \sum_{k\lambda} V_\lambda(k) [\hat{b}_{k\lambda 0}^\dagger + \hat{b}_{k\lambda 0}]$$

To further simplify the problem we consider a single mode carrying energy ω , fixed at the roton energy, and carrying angular momentum λ . The molecule-solvent interaction strength u is kept as a phenomenological parameter to be adjusted.

$$\hat{H} = B(\hat{\mathbf{L}} - \hat{\Lambda})^2 + \omega \sum_{\mu} \hat{b}_{\lambda\mu}^\dagger \hat{b}_{\lambda\mu} + u(\hat{b}_{\lambda 0}^\dagger + \hat{b}_{\lambda 0})$$

¹I.N. Cherepanov, GB, et al., Phys. Rev. A **104**, L061303 (2021).

²I.N. Cherepanov, GB, et al., New J. Phys. **24**, 075004 (2022).

³R. Schmidt and M. Lemeshko, Phys. Rev. X **6**, 011012 (2016).

Main results (1/2)

We diagonalize the Hamiltonian in the basis containing multiple excitations of the single bosonic mode:

$$\psi_{L[n_1 n_2 \dots n_m], M}^{(m)} = |LNM\rangle_{\text{mol}} \otimes \left(b_{\lambda n_1}^\dagger b_{\lambda n_2}^\dagger \dots b_{\lambda n_m}^\dagger |0\rangle_{\text{bos}} \right)$$

- Spectrum now includes a centrifugal distortion term

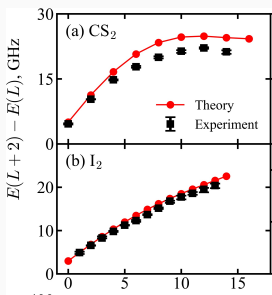
$$E_J = B^* J(J+1) - D^* J^2(J+1)^2$$

and now $E_L - E_{L-2} \propto \text{constant}$ in some region and can explain the observed spectrum.

- B^* and D^* are given in terms of simple analytical formulas

$$\frac{B^*}{B} \approx 1 - \frac{\tilde{u}^2}{(1 + \tilde{\omega})^3}; \quad \frac{D^*}{B} \approx \frac{\tilde{u}^2}{\lambda(\lambda + 1)(1 + \tilde{\omega})^5}$$

and the spectrum convincingly matches the experiments, up to high rotational states, for different molecules (CS_2 , I_2).



¹A.S. Chatterley, ..., GB, et al., Phys. Rev. Lett. **125**, 013001 (2020).

²I.N. Cherepanov, GB, et al., Phys. Rev. A **104**, L061303 (2021).

Main results (2/2)

- Empirical relationship

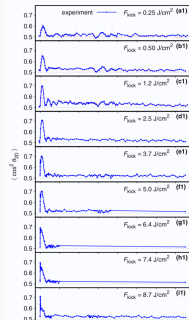
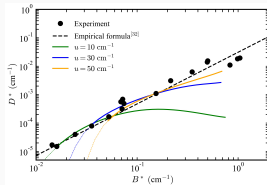
$$D^*/B \approx \xi (1 - B^*/B)^{5/3}$$

with $\xi = \tilde{u}^{-4/3}/[\lambda(\lambda + 1)]$. This dependence is similar to the power law

$$D^* = 0.031 \times B^{*1.818}$$

found on empirical grounds, but gives the correct limit when $B^* \rightarrow B$.

- Environment limited rotation: after a certain molecule-dependent value of L , the molecule loses energy to the environment very fast. Rotational analog or Landau's critical velocity?
- Timescales (a few ps vs. 450 fs).



^aA.S. Chatterley, ..., GB, et al., Phys. Rev. Lett. **125**, 013001 (2020).

^bI.N. Cherepanov, GB, et al., Phys. Rev. A **104**, L061303 (2021).

^cI.N. Cherepanov, GB, et al., New J. Phys. **24**, 075004 (2022).

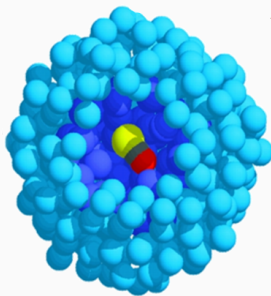
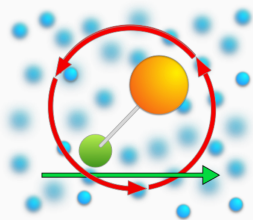
^dA. Cappellaro, GB, et al., J. Chem. Phys. **162**, 074104 (2025).

In this talk...

Rotating quantum impurities as quasiparticles, and diagrammatics

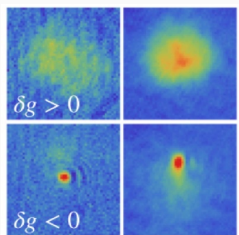
Molecules in ^4He nanodroplets

Ultra-cold atoms: an impurity in a Bose-Bose mixture



Images from S. Grebenev *et al.*, Science **279**, 2083 (1998) and from C.R. Cabrera's Ph.D. thesis.

An impurity in a heteronuclear two-component Bose-Bose mixture



C. D'Errico *et al.*,
Phys. Rev. Research **1**, 033155 (2019).

A **Bose-Bose mixture** consists of a mixture of two different bosonic atomic species.

Quite involved phase diagram in the ultracold regime, including the remarkable **quantum droplet** state, i.e. a liquid-like self-bound state.

Quantum droplets have been observed in a homonuclear spin mixture of ^{39}K , both in the presence of an external potential and in free space, as well as in a **heteronuclear mixture of ^{41}K and ^{87}Rb** .

We consider this system, plus one (structureless, pointlike) impurity.

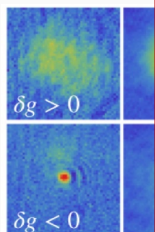
An impurity in a heteronuclear two-component Bose-Bose mixture

A **Bose-Bose mixture** consists of a mixture of two

What makes a **liquid** a
liquid?

Typically, it is a **balance**
between repulsive and
attractive interatomic
forces!

How can one achieve this
balance with **ultracold**
matter?



C. D'Errico *et al.*,
Phys. Rev. Research 1,

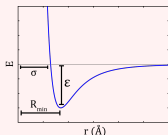


Image from: Wikibooks,
“Molecular simulation”.

old regime,
state, i.e. a

homonuclear
for an external
heteronuclear

else,

The system: Hamiltonian

Interacting Bose-Bose mixture:

$$\hat{H}_{\text{bb}} = \int d^3r \sum_{i=1,2} \hat{\phi}_i^\dagger(\mathbf{r}) \left(-\frac{\hbar^2 \nabla^2}{2m_i} + \frac{g_{ii}}{2} |\hat{\phi}_i(\mathbf{r})|^2 \right) \hat{\phi}_i(\mathbf{r}) + g_{12} \int d^3r |\hat{\phi}_1(\mathbf{r})|^2 |\hat{\phi}_2(\mathbf{r})|^2$$

where $\hat{\phi}_i, \hat{\phi}_i^\dagger$ ($i = 1, 2$) are bosonic field operators acting on two different bosonic species, m_i are the masses of each species and g_{ij} is the contact interaction strength between species i and species j .

Impurity in the mixture:

$$\hat{H}_{\text{I}} = \frac{\hat{\mathbf{P}}^2}{2m_{\text{I}}} + \sum_i g_{Ii} \int d^3r \rho(\mathbf{r}) |\hat{\phi}_i(\mathbf{r})|^2$$

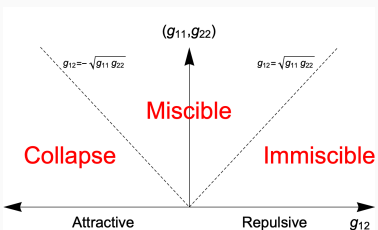
where g_{Ii} is the interaction between the impurity and the species i and $\rho(\mathbf{r}) = \delta^{(3)}(\mathbf{r} - \hat{\mathbf{R}})$.

Many parameters! Five different interaction strengths: $g_{11}, g_{22}, g_{12}, g_{I1}, g_{I2}$.

Bose-Bose mixture: mean-field phase diagram

Mean-field description: one can obtain conditions for the stability of the mixture at $T = 0$ from a Gross-Pitaevskii approach¹ considering $g_{11}, g_{22} > 0$ and varying the sign of g_{12} :

- When $g_{12} > \sqrt{g_{11}g_{22}}$ phase separation occurs.
- When $-\sqrt{g_{11}g_{22}} < g_{12} < \sqrt{g_{11}g_{22}}$ the system is in a miscible state.
- When $-\sqrt{g_{11}g_{22}} > g_{12}$ the system undergoes collapse.



¹See for instance C. Pethick and H. Smith, "Bose-Einstein condensation in dilute gases", (Cambridge University Press, Cambridge, England, 2002).

Self-bound quantum droplets in a Bose-Bose mixture

Single-component Bose gas

$$\frac{E}{V} = \frac{gn^2}{2} \left(1 + \frac{128\sqrt{na^3}}{15\sqrt{\pi}} + \dots \right)$$

with the LHY correction due to the zero-point motion of Bogoliubov excitation, i.e. a purely quantomechanical effect.

Two-component Bose mixture

$$\frac{E}{V} = \sum_{ij} \frac{g_{ij} n_i n_j}{2} + \frac{8}{15\pi^2} m_1^{3/2} (g_{11} n_1)^{5/2} f\left(\frac{m_2}{m_1}, \frac{g_{12}^2}{g_{11} g_{22}}, \frac{g_{22} n_2}{g_{11} n_1}\right)$$

and there can be competition between the mean-field attraction $\propto n^2$ and beyond mean-field repulsion $\propto n^{5/2}$, also in the weakly-interacting regime.

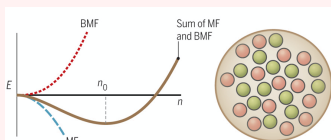
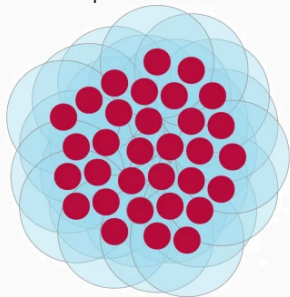


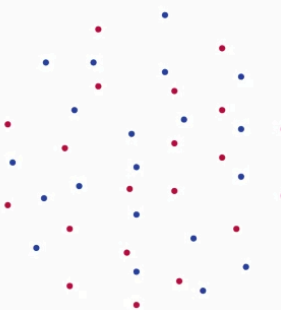
Image from: Science 359, 274 (2018).

Self-bound quantum droplets in a Bose-Bose mixture

“Classical” van der Waals paradigm
for a droplet



Quantum droplet



What about **dipolar droplets** (Dy in Stuttgart, Er in Innsbruck)? There are substantial differences, but the basic mechanism – mean-field attraction compensated by beyond-mean-field effects – is essentially the same.

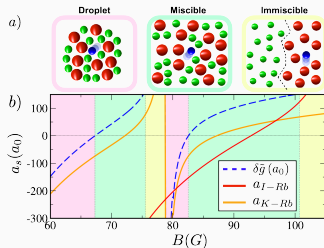
Images from D.S. Petrov, Nat. Phys. **14**, 211 (2018).

A closer look at the Bose-Bose mixture

We consider a **heteronuclear ^{41}K - ^{87}Rb Bose mixture**, on top of which we consider a dilute third component realized with a different hyperfine state of ^{41}K – which we shall dub the ‘I’ species. In the impurity limit for the third component, the system is described by five scattering lengths, namely $a_{\text{K-K}}$, $a_{\text{K-Rb}}$, $a_{\text{Rb-Rb}}$, $a_{\text{I-K}}$, $a_{\text{I-Rb}}$. The behaviour of $a_{\text{I-Rb}}$, and $a_{\text{K-Rb}}$ as a function of the magnetic field B in the range between 60 and 105 G.

The other three scattering lengths are almost constant in the range considered, i.e. $a_{\text{K-K}} \simeq a_{\text{I-K}} \simeq 62a_0$, $a_{\text{Rb-Rb}} \simeq 100.4a_0$.

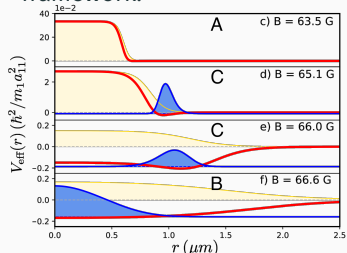
The liquid-gas transition parameter $\delta g = g_{\text{K-Rb}} + \sqrt{g_{\text{K-K}}g_{\text{Rb-Rb}}}$, allows us to chart the Bose mixture phase diagram: as the magnetic field is varied in the aforementioned range, the mixture goes through the droplet, miscible and immiscible phases.



Scattering length calculations: A. Simoni.

Droplet phase: results

We study the effect of an impurity in the droplet phase within the Gross-Pitaevskii framework.



Quite a rich phenomenology arises, with three different regimes.

A: for $B = 63.5 \text{ G}$ the potential, even though it has a small attractive region, does not support bound states in three dimensions not allowing for an impurity to be bound to the droplet.

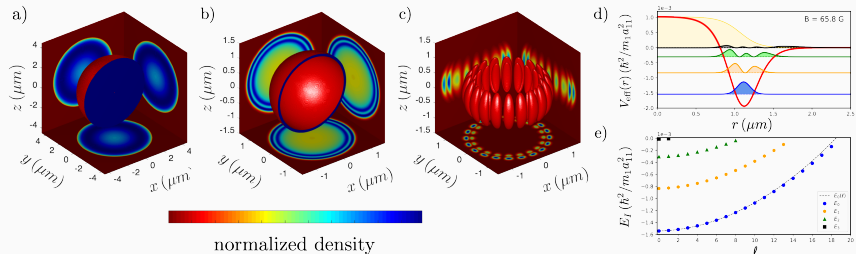
B: as the magnetic field is increased, for $B = 65.1 \text{ G}$ and for $B = 66.0 \text{ G}$ we observe that the impurity is localized at the surface of the droplet at a distance $r \approx 1 \mu\text{m}$ form the center.

C: finally, as the magnetic field is further increased we show that for $B = 66.6 \text{ G}$ the impurity is localized at the center of the self-bound droplet

GB, A. Burchianti, F. Minardi, T. Macrì, Phys. Rev. A **106**, 023301 (2022)

Rotational states: an impurity on the surface of a sphere?

Let us consider just the effective potential V_{eff} , for a fixed droplet profile. Which states can it support?



- a-b) Ground state of an impurity at $B = 66.6$ G and at $B = 65.8$ G.
- c) Excited state of an impurity at $B = 65.8$ G for $\ell = 10$ and $m = 10$.
- d) Effective potential $V_{\text{eff}}(r)$ and density of the impurity $n_I(r)$ for the $n = 0, \dots, 3$ s-wave bound states.
- e) Spectrum of the impurity eigenstates in the presence of the effective potential.

GB, A. Burchianti, F. Minardi, T. Macrì, Phys. Rev. A **106**, 023301 (2022)

A new perspective: **impurities on the surface of a sphere**. Experimental realization via a bubble trap in microgravity (fall tower, ISS)?

A new perspective: **impurities on the surface of a sphere**. Experimental realization via a bubble trap in microgravity (fall tower, ISS)?

How does the low-energy Hamiltonian look like?

$$\hat{H}_{\text{imp}} = \frac{\hbar^2 \hat{L}^2}{2mR^2}$$

$$\hat{H}_{\text{bos}} = \sum_{lm} \omega_l \hat{b}_{lm}^\dagger \hat{b}_{lm}$$

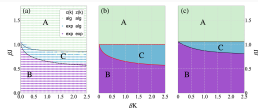
$$\hat{H}_{\text{imp-bos}} = \sum_{lm} U_{lm} Y_{lm}^*(\hat{\theta}_{\text{imp}}, \hat{\phi}_{\text{imp}}) b_{lm}^\dagger + h.c.$$

(Essentially) the same Hamiltonian as the one describing a rotating impurity in a 3D condensate. In one case the **topological information** is on the impurity, in the other case it is on the condensate, but the physics is the same!

Something more: multi-layer systems

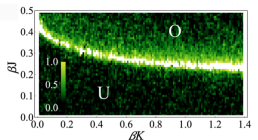
Classic bilayer XY model: **BKT-paired phase**.

$$\mathcal{H}_0 = -J \sum_{\langle ij \rangle} \cos(\phi_i - \phi_j) - J \sum_{\langle ij \rangle} \cos(\psi_i - \psi_j)$$
$$\mathcal{H}_1 = -K \sum_i \cos(\phi_i - \psi_i)$$



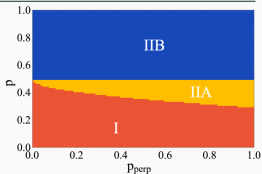
GB, N. Defenu, I. Nándori, L. Salasnich, A. Trombettoni, Phys. Rev. Lett. **123**, 100601 (2019).

Exotic phases in multi-layer systems can be discovered and categorized via **machine learning**.



W. Rządkowski, N. Defenu, S. Ciacchiera, A. Trombettoni, GB, New J. Phys. **22**, 093026 (2020).

Bond percolation on two-dimensional multilayers: p is the activation probability for intra-layer bonds, while p_{perp} is the activation probability for inter-layer bonds.



GB, A. Trombettoni, "Phase diagram of multilayer percolation", in preparation.

Acknowledgements

Diagrammatics and molecules in helium: Misha Lemeshko, Igor Cherepanov (IST Austria), Timur Tscherbul (U. Nevada, Reno), Alberto Cappellaro (Padova) and Henrik Stapelfeldt's group (Aarhus University).

Bose-Bose mixtures: Tommaso Macrì (Harvard, QuEra) Alessia Burchianti, Francesco Minardi (LENS, Florence).

Bilayers: Andrea Trombettoni (Trieste), Nicolò Defenu (ETH), Wojciech Rządkowski (Google).

Thank you for your attention.



Der Wissenschaftsfonds.



STRUCTURES
CLUSTER OF
EXCELLENCE



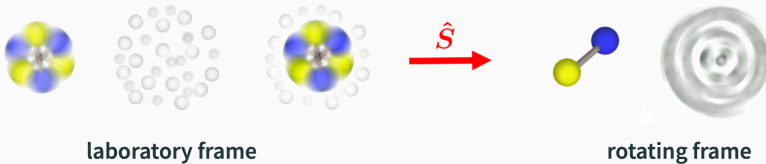
UNIVERSITÄT
HEIDELBERG
ZUKUNFT
SEIT 1386

Parts of this work are supported by a Lise Meitner Fellowship of the Austrian Science Fund (FWF), project Nr. M2461-N27 and by the DFG (German Research Foundation) under Germany's Excellence Strategy – the Heidelberg STRUCTURES Excellence Cluster.

These slides at <http://bigh.in>

Pekar Ansatz

Exact in the strong coupling regime.



Variational Ansatz

Expansion in bath excitations:

$$|\Psi\rangle \approx |\bullet\circlearrowleft\rangle_{\text{imp}} \otimes |0\rangle_{\text{bos}} + |\bullet\circlearrowright\rangle_{\text{imp}} \otimes |1\rangle_{\text{bos}} + \dots$$

Or, better, as the total angular momentum L, M is a good quantum number:

$$|\Psi_{LM}\rangle \approx |\bullet\circlearrowleft_{LM}\rangle_{\text{imp}} \otimes |0\rangle_{\text{bos}} + C_{j_1 m_1 j_2 m_2}^{LM} |\bullet\circlearrowright_{j_1 m_1}\rangle_{\text{imp}} \otimes |1_{j_2 m_2}\rangle_{\text{bos}} + \dots$$

plus some variational coefficients, to optimize by minimizing energy.

See for instance: R. Schmidt and M. Lemeshko, Phys. Rev. Lett. **114**, 203001 (2015).

Backup slide # 3

To study the effect of an impurity in the droplet phase we assume that, within the Gross-Pitaevskii framework, the two components are described by a single complex field $\phi(\mathbf{r})$ with the associated energy functional

$$\begin{aligned} E_{bb}[\phi_i] = & \int d^3r \sum_{i=1,2} \left(\frac{\hbar^2 |\nabla \phi_i|^2}{2m_i} + \frac{g_{ii}}{2} |\phi_i|^4 \right) + g_{12} |\phi_1|^2 |\phi_2|^2 + \\ & + \frac{8}{15\pi^2 \hbar^3} \left(m_1^{\frac{3}{5}} g_{11} |\phi_1|^2 + m_2^{\frac{3}{5}} g_{22} |\phi_2|^2 \right)^{\frac{5}{2}} \end{aligned}$$

where the last term is the beyond mean-field interaction for a general two-component mixture. The impurity interaction with the Bose mixture is described by the energy functional

$$E_I[\phi_i, \psi] = \int d^3r \frac{\hbar^2 |\nabla \psi|^2}{2m_I} + \left(g_{ID} |\phi(\mathbf{r})|^2 + \mathcal{E}_{\text{BMF}}(\mathbf{r}) \right) |\psi(\mathbf{r})|^2$$

The last term $\mathcal{E}_{\text{BMF}}(\mathbf{r})$ is the beyond mean-field interaction for a general two-component mixture. Note that $\mathcal{E}_{\text{BMF}} \propto n^{3/2}$.

Backup slide # 4

$$\begin{aligned}
 & \left\{ \begin{matrix} J_1 & J_2 & J_3 \\ J_{23} & J_{31} & J_{12} \end{matrix} \right\} \sum_{m_1 m_2 m_3} \binom{J_1 \quad J_2 \quad J_3}{m_1 \quad m_2 \quad m_3} D_{m_1 m'_1}^{J_1}(R_1) D_{m_2 m'_2}^{J_2}(R_2) D_{m_3 m'_3}^{J_3}(R_3) \\
 &= \sum_{\substack{M_{12} M_{23} M_{31} \\ M'_{12} M'_{23} M'_{31}}} (-1)^{J_{12}-M_{12}+J_{23}-M_{23}+J_{31}-M_{31}} \\
 &\times \binom{J_{12} \quad J_1 \quad J_{31}}{M_{12} \quad m'_1 - M'_{31}} \binom{J_{23} \quad J_3 \quad J_{13}}{M_{23} \quad m'_2 - M'_{12}} \binom{J_{31} \quad J_2 \quad J_{23}}{M_{31} \quad m'_3 - M'_{23}} \\
 &\times D_{M_{12} M'_{31}}^{J_{12}}(R_3^{-1} R_1) D_{M_{23} M'_{12}}^{J_{23}}(R_1^{-1} R_2) D_{M_{31} M'_{23}}^{J_{31}}(R_2^{-1} R_3).
 \end{aligned}$$

